CMLS, Cell. Mol. Life Sci. 62 (2005) 535–550
1420-682X/05/050535-16
DOI 10.1007/s00018-004-4305-7

CMLS Cellular and Molecular Life Sciences

Review

Study of molecular events in cells by fluorescence correlation spectroscopy

V. Vukojević [a,*], A. Pramanik [b], T. Yakovleva [a], R. Rigler [b], L. Terenius [a] and G. Bakalkin [a,*]

[a] Center for Molecular Medicine, Department of Clinical Neuroscience, Karolinska Institutet, S 171 76 Stockholm (Sweden), Fax: +46 8 517 761 80, e-mail: vladana.vukojevic@cmm.ki.se, e-mail: georgy.bakalkin@cmm.ki.se
[b] Department of Medical Biochemistry and Biophysics, Karolinska Institutet, S17176 Stockholm (Sweden)
Permanent address: Faculty of Physical Chemistry, University of Belgrade, Studentski trg 12-16, P. O. Box 137, 11001 Belgrade (Serbia and Montenegro)

Received 15 July 2004; received after revision 13 October 2004; accepted 12 November 2004

Abstract. To understand processes in a living cell, sophisticated and creative approaches are required that can be used for gathering quantitative information about large number of components interacting across temporal and spatial scales without major disruption of the integral network of processes. A physical method of analysis that can meet these requirements is fluorescence correlation spectroscopy (FCS), which is an ultrasensitive and non-invasive detection method capable of single-molecule and real-time resolution. Since its introduction about 3 decades ago, this until recently emerging technology has reached maturity. As commercially built equipment is now available, FCS is extensively applied for extracting biological information from living cells unattainable by other methods, and new biological concepts are formulated based on findings by FCS. In this review, we focus on examples in the field of molecular cellular biology. The versatility of the technique in this field is illustrated in studies of single-molecule dynamics and conformational flexibility of proteins, and the relevance of conformational flexibility for biological functions regarding the multispecificity of antibodies, modulation of activity of C5a receptors in clathrin-mediated endocytosis and multiplicity of functional responses mediated by the p53 tumor suppressor protein; quantitative characterization of physicochemical properties of the cellular interior; protein trafficking; and ligand-receptor interactions. FCS can also be used to study cell-to-cell communication, here exemplified by clustering of apoptotic cells via bystander killing by hydrogen peroxide.

Key words. Fluorescence correlation spectroscopy; cell biology; protein conformation; p53; intracellular transport; ligand-receptor interactions; apoptosis.

Introduction

If a picture is worth a thousand words, then nondestructive observation of molecules in living cells is priceless to cell biologists. Various fluorescence-microscopy-based techniques, such as fluorescence recovery after photobleaching (FRAP) [1–4], fluorescence loss in photobleaching (FLIP) [3], fluorescence resonance energy transfer (FRET) [1, 4, 5], fluorescence correlation spectroscopy (FCS) [6–10], multiple-photon excitation fluorescence microscopy (MPEFM) [11], fluorescence lifetime imaging microscopy (FLIM) [12], total internal reflection fluorescence microscopy (TIRFM) [13], and related techniques that have evolved in the past decade are, at the present time, probably the most sensitive techniques that can detect and identify molecules in the cell; measure local concentrations in different parts of cells; analyze molecular motion; detect chemical interactions

* Corresponding author.

and characterize them in terms of chemical thermodynamics and kinetics; and reveal single-molecule conformational transformations. As a result, the knowledge gathered by application of fluorescence microscopy-based techniques [14] in investigating cellular events has brought about new understanding of the cell structure and its complex dynamics at a molecular level.

The potential of FCS, which is non-invasive, has an ultimate detection limit of a single molecule and real-time resolution capacity, is not very widely appreciated. Therefore, we introduce here basic theoretical concepts of FCS and present breakthroughs in cellular molecular biology achieved by this approach in the past decade. Our aim is to show that FCS can be applied to study different aspects of cellular dynamics and to emphasize the importance of the biological information that was obtained.

FCS

The principles of FCS were formulated about 30 years ago [15–19] in the frame of a physical method called fluctuation correlation analysis. In this method statistical analysis of the time course and the amplitudes of spontaneous fluctuations in the number of particles occurring in a very small volume of a system is performed to derive conventional diffusion transport and chemical rate coefficients. Building on advantages of fluctuation correlation analysis and benefiting additionally from the high sensitivity and spectroscopic selectivity of fluorescence measurements, pioneers in the FCS field at Cornell University, Elliot Elson and Watt Webb and colleagues [15, 16, 18, 19], Måns Ehrenberg and Rudolf Rigler at the Karolinska Institute and Manfred Eigen at the Max Planck Institute [17, 20–22] developed a theoretical basis and built state-of-the-art equipment to perform delicate fluorescence fluctuation measurements, setting cornerstones not only for FCS but also for fluorescence photobleaching recovery [23–28], multiphoton FCS [29, 30] and multiphoton microscopy [31–33].

After its introduction in the seventies, the early use of FCS involved large excitation volumes and long correlation times, and the object was prone to photodestruction. Only after introducing technological improvements [19, 21, 22] did FCS acquire its present properties: single-molecule detection sensitivity and short measurement times, allowing studies of fast dynamic processes in living cells even if reporter molecules are present at low levels. In addition, recent advances and development of new techniques that enable protein labeling within cells, either by genetic fusion with fluorescent proteins or by labeling with small organic fluorophores [7, 34], further speeded up the rapid expansion of FCS applications in live cell studies.

Instrumentation and basic working principles

Instrumentation for FCS is nowadays commercially available from several manufacturers. A schematic presentation of a typical FCS setup is given in figure 1. To induce fluorescence, the sample is illuminated by incident light of a certain wavelength delivered by a laser. The laser beam is reflected by a dichroic mirror and sharply focused by the objective to form a miniature, yet very well defined volume element in the sample. The volume from which fluorescence is detected is further reduced by a pinhole (confocal aperture) in the image plane, to reject out-of-focus light and provide an elliptical volume element (fig. 1, insert; see appendix: Intensity detection function). This is crucial for providing a very small volume element (in today's equipment the observation volume from which fluorescence is detected is typically about 2×10^{-16} liters), and enables a submicrometer resolution facilitating detection at defined loci, as well as quantitative and background-free analysis.

Following the absorption of energy, fluorescent molecules lose energy through photon emission. The light emitted by fluorescing molecules passing through the confocal volume element is separated from the exciting radiation and the scattered light by a dichroic mirror and barrier filter, and transmitted to the detector, which responds with an electrical pulse to each detected photon. The number of pulses originating from the detected photons, recorded during a specific time interval, corresponds to the measured light intensity. Thus, in one experimental run we register changes in fluorescence intensity in time (fig. 1a).

To evaluate the gathered data, i.e. to analyze time series sampled at regular intervals during one run, statistical methods of data analysis are applied to detect non-randomness in the data. Typically, this is done by temporal autocorrelation analysis, but other ways of data analysis such as higher-order autocorrelation functions [35, 36], fluorescence intensity distribution analysis (FIDA) [37, 38], photon-counting histograms (PCHs) [39, 40] and recently developed fluorescence cumulant analysis (FCA) [41] can be also applied.

Temporal autocorrelation analysis of FCS data and interpretation

In temporal autocorrelation analysis we first derive the intensity autocorrelation function $C(t)$. $C(t)$ gives the correlation between the intensity of light, $I(t)$, measured at a certain time, t, and its intensity measured at a later time $t + \tau$, $I(t + \tau)$. The intensity autocorrelation function may be defined as an ensemble average:

$$C(\tau) = \langle I(t) I(t+\tau) \rangle \tag{1a}$$

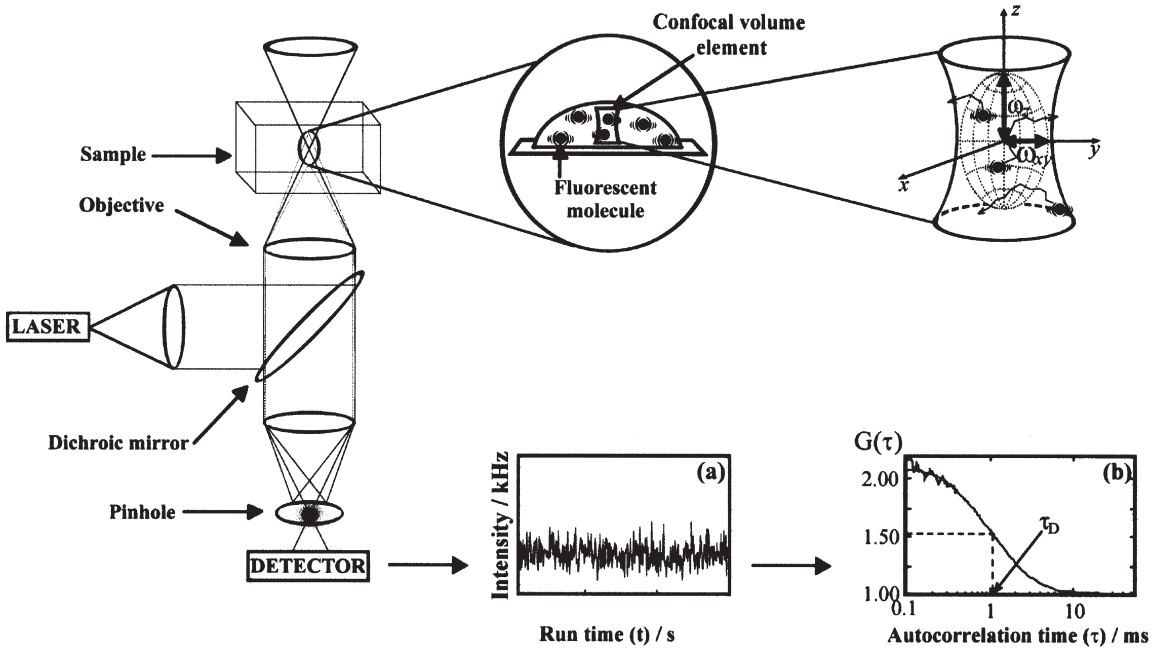

Figure 1. Schematic presentation of the instrumentation for FCS. (*a*) Light emitted by fluorescing molecules passing through the confocal volume element (the confocal volume element is magnified in the inserts) is transmitted to the detector, which responds with an electrical pulse to each detected photon. The number of pulses originating from the detected photons, recorded during a specific time interval, corresponds to the measured light intensity. Thus, in one experimental run we monitor how the intensity of fluorescence changes in time. (*b*) The electrical signal is gathered in regular time intervals, transferred to a digital signal correlation unit, and the corresponding normalized autocorrelation curve G(τ) is calculated on line. Autocorrelation function is fitted to the experimentally determined autocorrelation curve. In this particular example, the experimentally determined autocorrelation function is fitted with the three-dimensional diffusion autocorrelation function given in equation (3).

or, alternatively, as a time average of the product I(t) I(t + τ) measured over a certain accumulation time T:

$$C(\tau) = \lim_{T\to\infty} \frac{1}{T} \int_0^T I(t)I(t+\tau)dt \qquad (1b)$$

Since the unprocessed data in FCS are essentially fluorescence fluctuations over the mean fluorescence intensity ⟨I⟩, it is also possible to express the autocorrelation function through fluctuations of light intensities ∂I(t) = I(t) – ⟨I⟩ and ∂I(t + τ) = I(t + τ) – ⟨I⟩, at times t and t + τ, respectively. In this way, the intensity autocorrelation function is defined as:

$$C(\tau) = \langle I\rangle^2 + \langle \partial I(t)\partial I(t+\tau)\rangle \qquad (1c)$$

Regardless of the form of expression (1a)–(1c), as they are all equivalent, it is not convenient to use the intensity correlation function in practice because its value depends on properties of the applied experimental setup (see appendix: Intensity detection function). Therefore, instead of using the intensity autocorrelation function, it is more convenient to use the so-called normalized autocorrelation function, G(τ), defined as:

$$G(\tau) = 1 + \frac{\langle \partial I(t)\,\partial I(t+\tau)\rangle}{\langle I\rangle^2} \qquad (2a)$$

which is independent of properties as laser intensity, detection efficiency and fluorescence quantum yield.

For further analysis, the normalized autocorrelation function G(τ) has to be plotted for different lags, i.e. for different autocorrelation times τ. In molecular systems undergoing stochastic fluctuations, we observe random variations of G(τ) around the value G(τ) = 1. For processes that are not random, an autocorrelation curve is determined (fig. 1b). Typically, one observes a maximal limiting value of G(τ) as $\tau \to 0$, decreasing to the value of G(τ) = 1 at long times, indicating that correlation between the initial and the current property value has been lost. Very often only the so-called non-uniform part of the normalized autocorrelation function is analyzed. In this case one observes a maximal limiting value of G(τ) as $\tau \to 0$ that decreases to the value of G(τ) = 0 at long times. The limiting value of G(τ), as $\tau \to 0$, is then inversely proportional to the absolute concentration of the fluorescing molecules, as we shall show later.

Thereafter, the experimentally obtained autocorrelation curve has to be compared to autocorrelation functions derived for different model systems to identify an appropriate time series model. For example, if one fluorescent species is present in the sample and there are no intramolecular changes affecting the fluorescence of the observing molecules, the intensity fluctuations will re-

flect the passage of fluorescent particles through the observation volume. Since the passage of fluorescent particles is governed solely by diffusion, the best fitting of the autocorrelation curve (fig. 1 b) will be obtained by an autocorrelation function describing free diffusion of fluorescent particles [21]:

$$G(\tau) = 1 + \frac{1}{N} \cdot \frac{1}{\left(1 + \frac{\tau}{\tau_D}\right)\sqrt{1 + \frac{w_{xy}^2}{w_z^2}\frac{\tau}{\tau_D}}} \quad . \tag{3}$$

In equation (3) N is the average number of molecules in the observation volume, w_{xy} and w_z are radial and axial parameters, respectively, related to spatial properties of the detection volume (fig. 1, insert), τ is the autocorrelation time and τ_D is a characteristic decay time, typically called the diffusion time because it presents the average lateral transition time of the particle through the volume element. Spatial properties of the detection volume, represented in equation (3) by the square of the ratio of the radial and axial parameters $[(w_{xy}/w_z)^2]$, are determined experimentally in calibration measurements [42]. The calibration is performed in vitro, by using a solution of a dye for which the diffusion time (τ_D) is known. The autocorrelation curve derived in the calibration experiments is fitted by the autocorrelation function (3) using the known diffusion time (τ_D) of the dye, and the value of $(w_{xy}/w_z)^2$ is determined from the best-fitting curve.

The diffusion time, τ_D, of the investigated component is determined from the autocorrelation function (3) that best matches the actual, experimentally determined autocorrelation curve using the value for $(w_{xy}/w_z)^2$ determined from the calibration experiments. This parameter, derived directly from FCS measurements, is related to the translation diffusion coefficient D:

$$\tau_D = \frac{w_{xy}^2}{4D} \tag{4}$$

which is related to the size of the fluorescent molecules via the Stokes-Einstein equation:

$$D = \frac{kT}{6\pi\eta R} \tag{5}$$

In equation (5) k is the Boltzmann constant, T is absolute temperature, η is the solvent viscosity and R is the hydrodynamic radius of a hypothetical compact sphere in a viscous medium.*

Furthermore, as can be seen from equation (3), the limiting value of $G(\tau)$ as $\tau \to 0$ is related to the average number of molecules in the observation volume (N), i. e. it can be used to determine the absolute concentration (c) of the fluorescing molecules. For example, if $G(\tau) = 2.1$ at $\tau = 0$ (fig. 1 b), and the observation volume is $V = 2.0 \times 10^{-19}$ m^3, the concentration of the fluorescent molecules in the sample is $c = 7.5 \times 10^{-9}$ mol dm^{-3}.

Thus, although the measured fluctuations are utterly stochastic by themselves, their average rate of relaxation to the equilibrium value is not stochastic. Rather, it is constrained by macroscopic properties of the sample. And it is exactly this interrelation that makes it possible to apply fluctuation analysis to obtain information about physicochemical properties of the investigated system such as mobility coefficients, concentration, apparent hydrodynamic radius, chemical reaction constants and rates, binding and dissociation constants.

In cases other than the analyzed example of free diffusion of a single fluorescent species, the autocorrelation function attains forms different from the one given in equation (3) because all processes leading to statistical fluctuations in the fluorescence signal will induce a characteristic decay time in the autocorrelation curve. We give several examples of autocorrelation functions relevant in biological and biochemical applications in the appendix.

When applied in systems with more than one component, autocorrelation analysis has a practical detection limit that depends critically on the quantum yields, concentrations and differences in diffusion times of the molecules investigated [43]. For example, to distinguish two particles by the previously described second-order autocorrelation analysis of data, their diffusion times have to differ by a factor of 1.6 for bright fluorophores, or even more if they are less bright, meaning that their masses should differ about 5–8 times. Using data analysis techniques such as FIDA and PCH, which enable distinction of fluorescent species by differences in their molecular brightness and not by their diffusion coefficients, such obstacles can be overcome successfully, as was recently shown in in vivo protein interactions studies [44].

Physical cell biology approach by FCS

FCS is not merely a technique, but a rather general methodology effective in characterizing cellular processes on a molecular, subcellular, and intercellular level. In the following sections, we shall describe in more detail some applications of FCS that have impact for molecular and cellular biologists. Even though the selected topics are from diverse areas, they present only a fraction of work going on in the field of FCS. Therefore, to give a more complete overview of current achievements by FCS, we summarize references to related works in table 1.

* If the investigated molecule is of globular shape, its molecular mass (M) can be estimated from FCS measurements:

$$\frac{1}{D} \propto \frac{6\pi\eta}{kT} \cdot \sqrt[3]{M} \tag{5a}$$

Table 1. Recent reviews and applications of FCS in studies of biological systems.

Special scientific editions and reviews on FCS applications in biology
Biological Chemistry **382:** 2001
Fluorescence Correlation Spectroscopy: Theory and Applications, Rigler R. and Elson E. (eds), Springer, Berlin
Current Pharmaceutical Biotechnology **5** (2), 2004
[1], [7–10], [45–51]
Theoretical developments and advances
New concepts to measure fluorescence energy transfer via FCS [5]
Factors influencing FCS measurements on membranes [52]
Fractal analysis of fluorescence time series as a method to investigate anomalous diffusion [53]
Bias in FCS measurements [54]
Development toward application in highly heterogeneous systems [55]
Experimental artefacts in confocal FCS [56]
Concentration fluctuations in an oscillating chemical reaction system [57]
Standard deviation and accuracy in FCS [58]
High-order and dual-color correlation to probe non-equilibrium steady states [59]
Correction of artefacts in FCS measurements arising due to afterpulsing [60]
Unavoidable artefacts in FCS measurements due to photophysical properties of the fluorophore [61]
DNA structure and interactions
Dynamics of bubble formation in double-stranded DNA [62]
Dynamics of NCp7-mediated nucleic acid destabilization [63]
Formation and dissociation of the polyethylenimine/DNA complex [64]
Association of oligonucleotides with positively charged liposomes [65]
DNA looping by NgoMIV restriction endonuclease [66]
Dynamics of large semiflexible DNA chains [67]
Transport of nucleosome core particles in semidilute DNA solutions [68]
Rates of Mg^{2+} and Na^{+} dependent conformational changes in a single RNA molecule [69]
Denaturation of dsDNA by p53 [70]
Protein structure, interactions and function
Gag-Gag interactions during retrovirus assembly [71]
Stability of drug-induced tubulin rings [72]
Precipitation and size distribution of the Abeta(1)(-)(40) amyloid beta peptide in solutions [73]
Thermodynamic analysis of ssDNA-protein interaction [74]
Conformational dynamics and folding of the intestinal fatty acid binding protein [75]
Transportation of large transporting complex of tubulin [76]
Thrombin-induced fibrin polymerization [77]
p53 binding to double-stranded DNA oligonucleotides [78]
Ligand-receptor binding and diffusion
Binding of protoberberine type 2 alcaloids on the $GABA_A$ binding site [79]
Induction of seed germination via the strigolactone receptor [80]
Study of functional ribosomal complexes [81]
Protein incorporation in viral membranes [82]
Dynamics of ANS binding to tuna apomyoglobin [83]
Specific binding of proinsulin C-peptide to human skin fibroblasts [84]
Insulin binding to membrane receptors in renal tubular cells [85]
Applications in genetics
Gene expression analysis [86]
Integrin targeting for in vitro gene transfer [87]
Intracellular dynamics of a gene delivery vehicle [88]

Conformational fluctuations of single molecules

One central problem in molecular biology is to understand how the physicochemical properties of a single macromolecule determine its biological function in a living cell. Due to its submicrometer spatial resolution in two lateral directions (typically the detection volume is smaller than 0.5 μm × 0.5 μm × 2 μm), FCS may be performed on precisely defined locations, and may be exploited to detect individual macromolecules adsorbed or bound to surfaces, and track transformations as they perform their biological function. This strategy was applied in model systems to study the conformational dynamics of DNA oligomers [89], horseradish peroxidase (HRP) [90, 91] and flavin reductase [92] at the single-molecule level. Unlike the previously described diffusion experiments, in kinetic studies fluorescence fluctuations occur due to transitions between fluorescent and non-fluorescent states caused by a particular structural transformation or a chemical reaction. Kinetic parameters for the underlying process can be derived from the corresponding temporal autocorrelation functions [90, 93].

FCS experiments demonstrated that enzymatic activity of HRP on a single- molecule level varies broadly. To examine the origins of distributed kinetics in a single HRP

molecule, further analysis of data, in the form of higher-order correlation functions, was performed [91]. Such analysis indicated that widely distributed variation in enzymatic activity on a single-molecule scale appears because of alterations in molecular conformation arising due to thermodynamic fluctuations. This interpretation was later supported by theoretical analysis showing that intramolecular fluctuations appearing on a time scale shorter than the chemical reaction time scale may indeed result in rate coefficients that are different from average values observed for large number of molecules [94]. This means that HRP molecules exist in several thermodynamically slightly different conformations, and each conformation may show different enzymatic activity. For some conformations enzymatic activity is high, implying fast substrate turnover, whereas some conformations are inactive, i.e. they show no enzymatic function.

Besides showing widely distributed activity, correspondence between the conformation of a single HRP molecule and its past intercourse with the substrate was also revealed. This means that HRP molecules that were exposed to the substrate behave differently from molecules that were not exposed – HRP molecules that encountered the substrate more often attain the active conformation, whereas unexposed enzyme molecules attain any conformation from the set of conformational structures (the so-called ergodic assumption). Again, this was explained as a consequence of intramolecular transformation in a single HRP molecule.

These results have several important implications for cellular biology. First, it is important to establish whether conformational dynamics of a single HRP molecule influences its chemical performance at low concentrations only, as in the in vitro model, or also at higher concentrations relevant for subcellular organelles that are crowded by this and other macromolecules. What is the biological relevance of different conformers? Are they capable of catalyzing secondary reactions (catalytic promiscuity), or do they serve other functions that are not enzymatic, but may be structural or regulatory (a feature of proteins that is often referred to as moonlighting) [95]?

Second, they provide evidence for the long-existing hypothesis on protein structure that is nowadays known as the new view [96]. In contrast to the traditional standpoint on proteins as structurally restricted and functionally distinctive, the new view postulates the existence of proteins as an ensemble of conformational isomers [96–99]. Conformational isomers are characterized by similar, but distinctive values of relative Gibbs free energies and exist in an equilibrium state. Therefore, the free energy profile of the ensemble resembles a 'rugged energy landscape', rather than a smooth single well [100]. When the ligand binds to the protein, it binds predominantly to the conformer having the highest affinity. This disrupts the previously existing equilibrium, and the net reaction will be in a direction that tends to reduce the effect of ligand binding, i.e. it shifts the equilibrium in the direction of the formation of the conformer with the highest affinity for the ligand.

Conformational flexibility of proteins was invoked as regulatory mechanism in several recent studies. James et al. [99] have shown that the antibody SPE7 (a monoclonal immunoglobulin E (IgE) raised against a 2,4-dinitrophenyl hapten) can adopt at least two different conformations existing in an equilibrium state, that these conformations are independent of the presence of antigen and that each conformation can confer a different antigen-binding function. This is the first example of antibody multispecificity achieved through conformational diversity of the protein molecule. This strategy is biologically relevant because conformational isomers that adopt multiple functions increase the antibody repertoire.

In the FCS study of mechanisms by which activity of cell surface receptors is modulated in eukaryotic cells, a broad distribution of rate constants for trapping C5a receptors in clathrin-coated pits is suggested to be crucial for efficient clathrin-mediated endocytosis [101]. It is established that different conformational isomers of the receptor bind to the immobile cell component, with different rates creating a rugged energy landscape for binding, i.e. a multiple binding-unbinding equilibrium between the receptor and the immobile cell component. Again, conformational diversity enhances biological activity by allowing a broad distribution of residence times, ensuring efficient trapping of receptor proteins, and sufficient time for incorrectly targeted proteins to dissociate from the pit before it is internalized.

An FCS study of the p53 tumor suppressor protein resulted in a new model of activation of this latent transcription factor based on its conformational flexibility [102–104]. p53 activation leads to apoptosis or cell cycle arrest and is critical for cell differentiation and senescence. The choice of functional response appears to be determined by a subset of genes activated or inhibited by p53. Changes in protein conformation may attenuate p53 affinity for different types of DNA binding sites in the promoters of these subsets. Alternatively, distinct p53 conformations may be assumed upon binding to structurally diverse DNA target sequences [78, 103]. Allosterism of p53 target DNA sites has been described as sequence degeneracy, the variability in the number of half-sites composing these target sites, the different length of spacers connecting half-sites and the palindromic nature of these sites, allowing the formation of cruciform DNA structures [105–107]. It has been suggested that p53 in a conformation, bound to the 'inhibitory' sites, preferentially recruits histone deacetylase complexes [105] to chromatin, whereas p53 in a conformation, specific for the 'activatory' DNA complex, interacts predominantly with histone acetyltransferases. Accordingly, inhibition

of transcription by p53 is mediated by histone deacetylase mSin3a [108, 109], whereas p53 involves histone acetyltransferases such as p300/CBP, PCAF, TRRAP and ADA3 when it activates transcription [110–112]. Taken together, these data support the general model [103] postulating that p53 assumes different conformations when binding to DNA target sites with diverse topological properties. Distinct p53 conformations might favor the recruitment of specific coactivator constellations and corepressors, which would cooperatively modulate transcription of subsets of target genes critical for different physiological responses.

Finally, conformational diversity is not necessarily restricted to proteins, and may be relevant for other biomacromolecules [89]. Therefore, it is important to establish whether it is relevant in living cells, and in which way it may affect the biological functions of these molecules.

Quantitative characterization of cellular interior in living cells

Quantitative characterization of the heterogeneous cellular interior in physical and chemical terms is a prerequisite for understanding biological processes at a molecular level. Gathering information on physicochemical conditions in living cells, where molecular transformations and interactions take place in different phases, on phase boundaries, in crowded conditions, under concentration and electrostatic-potential gradients and fluxes of energy and matter, i.e. under conditions that are often far from thermodynamic equilibrium, is a first step towards a more comprehensive understanding of parameters governing chemical reactions in vivo. FCS is particularly useful in this respect, because it enables study of biochemical reactions in well-defined locations in intact cellular systems.

FCS was applied to determine the concentration, spatial localization and behaviour of reporter molecules in the cytoplasm [113, 114], membranes [19, 53, 82, 101, 115–118] and nuclei [119–122] in living cells. It was found that reporter protein molecules, labelled with small fluorescent molecules or fused with green-fluorescent protein (GFP), are generally subjected to drags that are 2–10 times larger, and diffuse at rates that are 40 to 100 times slower in cellular compartments compared to aqueous buffer solutions. Whether molecules experience larger drags in the cellular interior simply because of its increased apparent viscosity, or because of interactions with cellular elements, can be distinguished. In case of binding, fractions of bound and unbound reporters were determined.

There are many benefits from non-invasive local determination of physical and chemical properties of subcellular elements. For example, by measuring the diffusive properties of molecules, transient interactions, which are reflected in FCS measurements as anomalous diffusion (see e.g. [53] and references therein), may be revealed; by measuring drags experienced by molecules in different areas of the cytoplasm, such as the zone of cytoplasmic streaming, bulk cytoplasm and cytoplasm adjacent to cellular structures, local apparent viscosity of these regions could be determined, and cytoplasmic spatial inhomogeneity in terms of apparent viscosity could be mapped. Such information may be used in living cells to identify very fast, often diffusion-limited, transient reactions, estimate their rates and investigate how they change in cellular structures with different viscosities [97].

Another important point in determining local concentrations and diffusion rates is that we may begin to understand on a quantitative level how molecular crowding, local differences in pH, ionic strength and redox potentials influence the course of biochemical reactions [123, 124]. By distinguishing non-equilibrium steady states maintained through a continuous exchange of energy and matter from equilibrium states without flux [59] and by studying the interplay of diffusion and chemical kinetics in living cells, we may come closer to understanding how non-linear processes in non-equilibrium cellular environments lead to biological complexity: how it is possible to escape limitation by diffusion in the glucose phosphotransferase system in bacterial cells, and why this is not possible in eukaryotic cells [125], what critical number of molecules is required to establish cellular rhythms and how robust they are in respect to molecular noise [126, 127], how physicochemical mechanisms of self-organization lead to formation of spatial receptor-ligand synaptic patterns in the intercellular junctions (observed in T-cell/antigen-presenting cell junctions with different major histocompatibility complex peptides and in natural killer cells, for example) and what their role is in cell-cell interactions [128], and how non-linear mechanisms of spatiotemporal symmetry breaking lead to pattern formation in somitogenesis [129]. Understanding these cellular mechanisms at a molecular level is not an unrealistic goal, thanks to computational power and mathematical modeling [126, 127, 130–132]. However, to achieve it, meticulous experimental mapping of local conditions inside the cell has to be accomplished first.

Protein trafficking

The majority of soluble and membrane-bound macromolecules are transported from sites of their synthesis to locations in the cell where they perform their functions. The rate at which they migrate determines the rates of many biochemical reactions and may constrain a variety of cellular functions, as is well documented in the chemotactic response of *Escherichia coli* [123]. In addition, rates at which molecules migrate in living cells cannot be directly extrapolated from in vitro measurements [123].

Therefore it is important to measure such properties in vivo.

To investigate transport through the cytosol and plastids of plant cells, diffusion of GFP and GFP fused with a peptide that targets it to plastids was studied by FCS [133]. For fluorescence detection at a low scattering background and minimal interference with cell viability, a two-photon excitation of the dyes is used.* The FCS detection volume was focused on different positions within the cell to investigate protein motion in the cytosol and along the plastid stromule, and special attention was given to distinguish effects that arise due to differences in viscosities of these cellular structures from other interfering effects. It was established that GFP moves by free diffusion [eq. (3)] in the cytosol, and its diffusion coefficient is determined to be about 2–3 times smaller than in aqueous solutions. However, the flow characteristics of GFP fusion protein targeted to plastids through the plastid tubules (stromules) are not simple, and can be described by a mixed mode diffusion model having contributions from both free diffusion and active transport (see appendix, table A, AF8). It was determined that free diffusion in plastid tubules was about 50 times slower than in the cytosol, and about 100 times slower than in aqueous solutions, whereas the velocities of active transport and free diffusion of GFP molecules were determined to be comparable.

Besides being the first successful application of FCS to decouple passive diffusion from active transport [133], and setting an example for future applications, this work gives interesting insight into cellular transportation strategy. At short distances, the rate at which molecules migrate by active transport is comparable to that of free diffusion. However, active transport is apparently more efficient for long-distant transportation. Thus, it is advantageous to transport protein molecules from plastids to distant locations within the cell by active transport along plastid tubules, despite the energy requirements, whereas free diffusion is probably preferred for short-distance transportation within the cytosol.

Cell signaling and information exchange

Living cells exchange information through physicochemical processes that occur consecutively and/or in parallel at different levels of spatial organization and on a multitude of temporal scales. The involved events may be extremely fast and highly localized, e.g. binding of signal molecules to membrane receptors, or may be slower and spatially expanded, as in highly coordinated wave propagation and translocation of signaling molecules through the cellular interior [135].

FCS provides a unique opportunity to investigate different aspects of intra- and intercellular communication in vivo and in real time. To this end, FCS was applied successfully to extensively study ligand-receptor binding [136–146]: to investigate ligand-induced oligomerization and formation of specific somatostain receptors [147], expression and clustering of the ionotropic $5HT_3$ receptor in human embryonic kidney cells [82]; diffusion of PKCβI (a subtype of protein kinase C) in the cytosol and plasma membrane of human embryonic kidney cells, and mechanisms of its translocation and anchoring [114]; and mechanisms for trapping transmembrane G protein-coupled receptors during endocytosis [101].

Having generated individual results and characterized ligand-receptor binding kinetics [142], determined the status of receptors [146], investigated mechanisms of their translocation [114], determined properties and composition of membranes in which receptors are embedded [148], and assessed how local membrane topography and composition influences apparent mobility of receptors [53], we may integrate these results into a coherent framework and acquire a deeper understanding of how these properties, which are intricately coupled and superimposed one on another in living cells, influence the outcome of internal cell-signaling pathways.

Peroxide-induced apoptosis in bystander cells

In the above-mentioned examples the FCS approach based on temporal autocorrelation analysis was used to investigate properties of the reporter molecules, which were either endogenously fluorescent or were fluorescently labeled. An alternative approach is to use the ultrasensitivity of the FCS equipment and its capacity for very fast measurements to monitor the formation of a fluorescent reporter that is being formed upon interactions with the non-fluorescent compound of interest. Such an approach was utilized to study intercellular communication in bystander cell killing in real time [149].

The phenomenon of bystander killing was first observed in cell cultures in vitro, when it was noticed that cells killed individually by exposure to α-particles or X-rays increase the incidence of apoptosis in non-hit bystander cells [150–152]. To examine the mechanisms, a model of bystander-cell killing in cell monolayers was developed [149]. When spontaneous apoptosis occurred, or when cell death was triggered by deprivation of growth factors or expression of the p53 tumor suppressor protein, clusters of apoptotic cells were formed, suggesting that dying cells emit chemical death signals that kill viable by-

* In two-photon excitation FCS [29, 30, 45, 134], excitation occurs by simultaneous absorption of two photons (time span between absorption events is less than 10^{-15} s). Excitation occurs in a precisely defined subfemtoliter focal volume, where the focused light intensity is high enough to allow simultaneous absorption. Two-photon excitation FCS does not require confocal detection, and provides for higher penetration depth in biological tissue and lower phototoxicity.

standers. Synchronization of apoptosis in a limited group of adjacent cells suggests that the half-life of the emitted death substance is roughly in the order of time required for its diffusion across cell clusters. This notion limited the number of possible substances to NO and H_2O_2, which are known to have a half-life in the order of seconds, are toxic and easily diffuse through cell membranes. To distinguish between them, the influence of NO and H_2O_2 inhibitors on bystander killing was examined. Cell clustering was inhibited by catalase, an enzyme known to be peroxide scavenger, whereas it was unaffected by NO inhibitors, suggesting that H_2O_2 functions as an extracellular cell-death signal.

The FCS instrument was applied to identify and quantify the amount of H_2O_2 through its capacity to oxidize the trapped non-fluorescent 5-(and-6)-carboxy-2′,7′-dichlorodihydro-fluorescein and produce a fluorescent reporter 5-(and-6)-carboxy-2′,7′-dichloro-fluorescein with a characteristic fluorescence spectrum [149]. Fluorescence intensities were measured by the FCS instrument, and the amount of H_2O_2 was evaluated from a calibration curve [149]. In this example, autocorrelation analysis was not performed because it would give information about diffusion properties of the reporter molecule which is not relevant for the problem considered. These experiments demonstrated that viable cells emit low levels of H_2O_2, whereas the dying apoptotic cells generate 100–1000-fold higher amounts of this toxic compound. Average H_2O_2 levels inside apoptotic cells (2 µm below the cell surface) were similar to that at the cell surface, whereas in the surrounding medium a H_2O_2 concentration gradient was observed, with the highest level at the cell surface (table 2). Thus, peroxide was apparently produced inside apoptotic cells, and released into the extracellular medium.

Peroxide concentrations inside apoptotic cells and in the nearby medium are determined to be in the range of those released by activated macrophages and neutrophils, which are as high as 5–10 µM [153–155], and the cumulative concentration released by apoptotic cells is apparently sufficient to kill viable bystanders.

These findings raise several important questions. First of all, why do apoptotic cells produce a toxic substance? Does the spatial distribution of the released toxic compound have a purpose in cell-cell interactions that is yet unknown? Is clustering of apoptotic cells a general phenomenon characteristic for normal tissue during development, and pathological conditions when massive cell death is induced by toxic influences or tissue damage?

Table 2. Levels of hydrogen peroxide generated by apoptotic cells and emitted to the surroundings.

Cell	Laser focus	$[H_2O_2]$/µM
Viable	intracellular	0.05 ± 0.04
Apoptotic	intracellular	14 ± 4
	10 µm above the cell surface	7 ± 3
	20 µm above the cell surface	2.0 ± 0.5
Culture medium	at distance from the cell surface	1.5 ± 0.5

Concluding remarks

In the past few years speed, sensitivity and time resolution of FCS measurements have been considerably enhanced. FCS has thus risen from a technique valued for its ability to detect and identify sparse molecules, which is important for analytical purposes and medical diagnostics [46, 156–159], to a very powerful methodological approach to tackle basic problems in cell biology. Extending the classical temporal autocorrelation FCS to dual-color cross-correlation analysis [160–165], spatially resolved analysis [121], fluorescence intensity analysis [166] and fluorescence intensity and lifetime distribution analysis [167], and combination with other techniques such as multiple-photon microscopy and imaging [33, 113, 134], fluorescent resonance energy transfer [165], total internal reflection [23, 68, 101] and second harmonic generation microscopy [32, 169] will expand the potential of FCS for biological applications even further.

Acknowledgement. We wish to thank Dr Joseph Schlessinger at Yale University for critical reading of the manuscript. This work was supported by grants from the Swedish Cancer Society, Swedish Science Research Council and AFA Foundations to G.B. and the Wenner-Gren Foundations to V.V.

1 Lippincott-Schwartz J., Snapp E. and Kenworthy A. (2001) Studying protein dynamics in living cells. Nat. Rev. Mol. Cell Biol. **2:** 444–456
2 Reits E. A. J. and Neefjes J. J. (2001) From fixed to FRAP: measuring protein mobility and activity in living cells. Nat. Cell Biol. **3:** E145–E147
3 Klonis N., Rug M., Harper I., Wickham M., Cowman A. and Tilley L. (2002) Fluorescence photobleaching analysis for the study of cellular dynamics. Eur. Biophys. J. **31:** 36–51
4 Roy P., Rajfur Z., Pomorski P. and Jacobson K. (2002) Microscope based techniques to study cell adhesion and migration. Nat. Cell Biol. **4:** E91–E96
5 Widengren J., Schweinberger E., Berger S. and Seidel C. A. M. (2001) Two new concepts to measure fluorescence energy transfer via fluorescence correlation spectroscopy: theory and experimental realization. J. Phys. Chem. A **105:** 6851–6866
6 Webb W. W. (2001) Fluorescence correlation spectroscopy: genesis, evolution, maturation and prognosis. In: Fluorescence Correlation Spectroscopy. Theory and Applications, pp. 305–330, Rigler R. and Elson E. L. (eds), Springer, Berlin
7 Bacia K. and Schwille P. (2003) A dynamic view of cellular processes by in vivo fluorescence auto- and cross-correlation spectroscopy. Methods **29:** 74–85
8 Haustein E. and Schwille P. (2003) Ultrasensitive investigation of biological systems by fluorescence correlation spectroscopy. Methods **29:** 153–166

9 Hink M. A., Borst J. W. and Visser A. J. (2003) Fluorescence correlation spectroscopy of GFP fusion proteins in living plant cells. Methods Enzymol. **361:** 93–113
10 Müller J. D., Chen Y. and Gratton E. (2003) Fluorescence correlation spectroscopy. Methods Enzymol. **361:** 69–92
11 Cannon D. M. Jr, Winograd N. and Ewing A. G. (2000) Quantitative chemical analysis of single cells. Annu. Rev. Biophys. Biomol. Struct. **29:** 239–263
12 Cubeddu R., Comelli D., D'Andrea C., Taroni P. and Valentini G. (2002) Time-resolved fluorescence imaging in biology and medicine. J. Phys. D: Appl. Phys. **35:** R61–R76
13 Axelrod D. (2003) Total internal reflection fluorescence microscopy in cell biology. Methods Enzymol. **361:** 1–33
14 Diaspro A. (ed.) (2001) Confocal and Two-Photon Microscopy: Foundations, Applications and Advances, Wiley-Liss, New York
15 Magde D., Webb W. W. and Elson E. (1972) Thermodynamic fluctuations in a reacting system – measurement by fluorescence correlation spectroscopy. Phys. Rev. Lett. **29:** 705–708
16 Elson E. L. and Magde D. (1974) Fluorescence correlation spectroscopy. Conceptual basis and theory. Biopolymers **13:** 1–27
17 Ehrenberg M. and Rigler R. (1974) Rotational Brownian motion and fluorescence intensity fluctuations. Chem. Phys. **4:** 390–401
18 Koppel D. E. (1974) Statistical accuracy in fluorescence correlation spectroscopy. Phys. Rev. A **10:** 1938–1945
19 Koppel D. E., Axelrod D., Schlessinger J., Elson E. L. and Webb W. W. (1976). Dynamics of fluorescence marker concentration as a probe of mobility. Biophys. J. **16:** 1315–1329
20 Ehrenberg M. and Rigler R. (1972) Polarized fluorescence and rotational Brownian motion. Chem. Phys. Lett. **14:** 539–544
21 Rigler R., Mets Ü., Widengren J. and Kask P. (1993) Fluorescence correlation spectroscopy with high count rate and low background. Eur. Biophys. J. **22:** 169–175
22 Eigen M. and Rigler R. (1994) Sorting single molecules: application to diagnostics and evolutionary biotechnology. Proc. Natl. Acad. Sci. USA **91:** 5740–5747
23 Axelrod D., Koppel D. E., Schlessinger J., Elson E. and Webb W. W. (1976) Mobility measurement by analysis of fluorescence photobleaching recovery kinetics. Biophys. J. **16:** 1055–1069
24 Elson E. L., Schlessinger J., Koppel D. E., Axelrod D. and Webb W. W. (1976) Measurement of lateral transport on cell surfaces. Prog. Clin. Biol. Res. **9:** 137–147
25 Schlessinger J., Koppel D. E., Axelrod D., Jacobson K., Webb W. W. and Elson E. L. (1976) Lateral transport on cell membranes: mobility of concanavalin A receptors on myoblasts. Proc. Natl. Acad. Sci. USA **73:** 2409–2413
26 Schlessinger J., Axelrod D., Koppel D. E., Webb W. W. and Elson E. L. (1977) Lateral transport of a lipid probe and labeled proteins on a cell membrane. Science **195:** 307–309
27 Jacobson K., Elson E., Koppel D. and Webb W. W. (1982) Fluorescence photobleaching in cell biology. Nature **295:** 283–284
28 Yechiel E. and Edidin M. (1987) Micrometer-scale domains in fibroblast plasma membranes. J. Cell Biol. **105:** 755–760
29 Berland K. M., So P. T. C. and Gratton E. (1995) Two-photon fluorescence correlation spectroscopy: method and application to the intracellular environment. Biophys. J. **68:** 694–701
30 Schwille P., Haupts U., Maiti S. and Webb W. W. (1999) Molecular dynamics in living cells observed by fluorescence correlation spectroscopy with one- and two-photon excitation. Biophys. J. **77:** 2251–2265
31 Denk W., Strickler J. H. and Webb W. W. (1990) Two-photon laser scanning fluorescence microscopy. Science **248:** 73–76
32 Zipfel W. R., Williams R. M., Christie A., Nikitin A.Y., Hyman B. T. and Webb W. W. (2003) Live tissue intrinsic emission microscopy using multiphoton-excited native fluorescence and second harmonic generation. Proc. Natl. Acad. Sci. USA **100:** 7075–7080
33 Zipfel W. R., Williams R. M. and Webb W. W. (2003) Nonlinear magic: multiphoton microscopy in the biosciences. Nat. Biotech. **21:** 1369–1377
34 Miyawaki A., Sawano A. and Kogure T. (2003) Lighting up cells: labelling proteins with fluorophores. Nat. Cell Biol. **Suppl.:** S1–S7
35 Thompson N. L. (1991) Fluorescence correlation spectroscopy. In: Topics in Fluorescence Spectroscopy, Vol. 1, Techniques, pp. 337–378, Lakowicz J. R. (ed.), Plenum Press, New York
36 Qian H. and Elson E. L. (1990) On the analysis of high order moments of fluorescence fluctuations. Biophys. J. **57:** 375–380
37 Kask P., Palo K., Ullmann D. and Gall K. (1999) Fluorescence-intensity distribution analysis and its application in biomolecular detection technology. Proc. Natl. Acad. Sci. USA **96:** 13756–13761
38 Kask P., Palo K., Fay N., Brand L., Mets U., Ullmann D. et al. (2000) Two-dimensional fluorescence intensity distribution analysis: theory and applications. Biophys J. **78:** 1703–1713
39 Chen Y., Müller J. D., So P. T. C and Gratton E. (1999) The photon counting histogram in fluorescence fluctuation spectroscopy. Biophys. J. **77:** 553–567
40 Hillesheim L. N. and Müller J. D. (2003) The photon counting histogram in fluorescence fluctuation spectroscopy with non-ideal photodetectors. Biophys. J. **85:** 1948–1958
41 Müller J. D. (2004) Cumulant analysis in fluorescence fluctuation spectroscopy. Biophys. J. **86:** 3981–3992
42 Weisshart K., Jüngel V. and Briddon S. J. (2004) The LSM 510 META-ConfoCor 2 system: an integrated imaging and spectroscopic platform for single-molecule detection. Curr. Pharm. Biotechnol. **5:** 135–154
43 Meseth U., Wohland T., Rigler R. and Vogel H. (1999) Resolution of fluorescence correlation measurements. Biophys. J. **76:** 1619–1631
44 Chen Y., Wei L. N. and Müller J. D. (2003) Probing protein oligomerization in living cells with fluorescence fluctuation spectroscopy. Proc. Natl. Acad. Sci. USA **100:** 15492–15497
45 Schwille P. (2001) Fluorescence correlation spectroscopy and its potential for intracellular applications. Cell. Biochem. Biophys. **34:** 383–408
46 Földes-Papp Z., Demel U. and Tilz G. P. (2001) Ultrasensitive detection and identification of fluorescent molecules by FCS: Impact for immunology. Proc. Natl. Acad. Sci. USA **98:** 11509–11514
47 Hess S. T., Huang S., Heikal A. A. and Webb W. W. (2002) Biological and chemical applications of fluorescence correlation spectroscopy: a review. Biochemistry **41:** 697–705
48 Thompson N. L., Lieto A. M. and Allen N. W. (2002) Recent advances in fluorescence correlation spectroscopy. Curr. Opin. Struc. Biol. **12:** 634–641
49 Hink M. A., Bisseling T. and Visser A. J. W. G. (2002) Imaging protein – protein interactions in living cells. Plant Mol. Biol. **50:** 871–883
50 Elson E. L. (2001) Fluorescence correlation spectroscopy measures molecular transport in cells. Traffic **2:** 789–796
51 Pramanik A. and Widengren J. (2004) Fluorescence correlation spectroscopy (FCS). In: Encyclopedia of Molecular Cell Biology and Molecular Medicine, vol. 4, pp. 461–499, Meyers R. A. (ed.), Wiley, New York
52 Milon S., Hovius R., Vogel H. and Wohland T. (2003) Factors influencing fluorescence correlation spectroscopy measurements on membranes: simulations and experiments. Chem. Phys. **288:** 171–186
53 Weiss M., Hashimoto H. and Nilsson T. (2003) Anomalous protein diffusion in living cells as seen by fluorescence correlation spectroscopy. Biophys. J. **84:** 4043–4052

54 Saffarian S. and Elson E. L. (2003) Statistical analysis of fluorescence correlation spectroscopy: the standard deviation and bias. Biophys. J. **84:** 2030–2042
55 Sengupta P., Garai K., Balaji J., Periasamy N. and Maiti S. (2003) Measuring size distribution in highly heterogeneous systems with fluorescence correlation spectroscopy. Biophys. J. **84:** 1977–1984
56 Hess S. T. and Webb W. W. (2002) Focal volume optics and experimental artefacts in confocal fluorescence correlation spectroscopy. Biophys. J. **83:** 2300–2317
57 Qian H., Saffarian S. and Elson E. L. (2002) Concentration fluctuations in a mesoscopic oscillating chemical reaction system. Proc. Natl. Acad. Sci. USA **99:** 10376–10381
58 Wohland T., Rigler R. and Vogel H. (2001) The standard deviation in fluorescence correlation spectroscopy. Biophys. J. **80:** 2987–2999
59 Qian H. and Elson E. L. (2004) Fluorescence correlation spectroscopy with high-order and dual-color correlation to probe nonequilibrium steady states. Proc. Natl. Acad. Sci. USA **101:** 2828–2833
60 Zhao M., Jin L., Chen B., Ding Y., Ma H. and Chen D. (2003) Afterpulsing and its correction in fluorescence correlation spectroscopy experiments. Appl. Opt. **42:** 4031–4036
61 Nishimura G. and Kinjo M. (2004) Systematic error in fluorescence correlation measurements identified by a simple saturation model of fluorescence. Anal. Chem. **76:** 1963–1970
62 Altan-Bonnet G., Libchaber A. and Krichevsky O. (2003) Bubble dynamics in double-stranded DNA. Phys. Rev. Lett. **90:** 138101
63 Azoulay J., Clamme J.-P., Darlix J.-L., Roques B. P. and Mély Y. (2003) Destabilization of the HIV-1 complementary sequence of TAR by the nucleocapsid protein through activation of conformational fluctuations. J. Mol. Biol. **326:** 691–700
64 Clamme J.-P., Azoulay J. and Mély Y. (2003) Monitoring of the formation and dissociation of polyethylenimine/DNA complex by two-photon fluorescence correlation spectroscopy. Biophys. J. **84:** 1960–1968
65 Jurkiewicz P., Okruszek A., Hof M. and Langner M. (2003) Associating oligonucleotides with positively charged liposomes. Cell. Mol. Biol. Lett. **8:** 77–84
66 Katiliene Z., Katilius E. and Woodbury N. W. (2003) Single molecule detection of DNA looping by NgoMIV restriction endonuclease. Biophys. J. **84:** 4053–4061
67 Lumma D., Keller S., Vilgis T. and Radler J. O. (2003) Dynamics of large semiflexible chains probed by fluorescence correlation spectroscopy. Phys. Rev. Lett. **90:** 218301
68 Mangenut S., Keller S. and Rädler J. (2003) Transport of nucleosome core particles in semidilute DNA solutions. Biophys. J. **85:** 1817–1825
69 Kim H. D., Nienhaus U. G., Ha T., Orr J. W., Williamson J. R. and Chu S. (2002) Mg^{2+}-dependent conformational change of RNA studied by fluorescence correlation and FRET on immobilized single molecules. Proc. Natl. Acad. Sci. USA **99:** 4284–4289
70 Vukojević V., Yakovleva T., Terenius L., Pramanik A. and Bakalkin G. (2004) Denaturation of dsDNA by p53: fluorescence correlation spectroscopy study. Biochem. Biophys. Res. Commun. **316:** 1150–1155
71 Larson D. R., Ma Y. M., Vogt V. M. and Web W. W. (2003) Direct measurement of Gag-Gag interaction during retrovirus assembly with FRET and fluorescence correlation spectroscopy. J. Cell Biol. **162:** 1233–1244
72 Boukari H., Nossal R. and Sackett D. L. (2003) Stability of drug-induced tubulin rings by fluorescence correlation spectroscopy. Biochemistry **42:** 1292–1300
73 Sengupta P., Garai K., Sahoo B., Shi Y., Callaway D. J. and Maiti S. (2003) The amyloid beta peptide (Abeta(1)(-)(40)) is thermodynamically soluble at physiological concentrations. Biochemistry **42:** 10506–10513
74 Schubert F., Zettl H., Hafner W., Krauss G. and Krausch G. (2003) Comparative thermodynamic analysis of DNA-Protein interactions using surface plasmon resonance and fluorescence correlation spectroscopy. Biochemistry **42:** 10288–10294
75 Chattopadhyay K., Saffariab S., Elson E. L. and Frieden C. (2002) Measurement of microsecond dynamic motion in the intestinal fatty acid binding protein by using fluorescence correlation spectroscopy. Proc. Natl. Acad. Sci. USA **99:** 14171–14176
76 Terada S., Kinjo M. and Hirokawa N. (2000) Oligomeric tubulin in large transporting complex is transported via kinezin in squid giant axons. Cell **103:** 141–155
77 Bark N., Földes-Papp Z. and Rigler R. (1999) The incipient stage in thrombin-induced fibrin polymerisation detected by FCS at the single molecule level. Biochem. Biophys. Res. Commun. **260:** 35–41
78 Wölcke J., Reimann M., Klumpp M., Göhler T., Kim E. and Deppert W. (2003) Analysis of p53 'latency' and 'activation' by fluorescence correlation spectroscopy: evidence for different modes of high affinity DNA binding. J. Biol. Chem. **278:** 32587–32595
79 Halsbugth C., Meissner O. and Häberlein H. (2003) Positivie cooperation of protoberberine type 2 alcaloids from *Corydalis cava* on the $GABA_A$ binding site. Planta Med. **69:** 305–309
80 Reizelman A., Wigchert S. C., del-Bianco C. and Zwanenburg B. (2003) Synthesis and bioactivity of labelled germination stimulants for the isolation and identification of the strigolactone receptor. Org. Biomol. Chem. **1:** 950–959
81 Jermutus L., Kolly R., Földes-Papp Z., Hanes J., Rigler R. and Plückthun A. (2002) Ligand binding of a ribosome-displayed protein detected in solution at the single molecule level by fluorescence correlation spectroscopy. Eur. Biophys. J. **31:** 179–184
82 Pick H., Preuss A. K., Mayer M., Wohland T., Hovius R. and Vogel H. (2003) Monitoring expression and clustering of the ionotropic 5HT3 receptor in plasma membranes of live biological cells. Biochemistry **42:** 877–884
83 Bismuto E., Gratton E. and Lamb D. C. (2001) Dynamics of ANS binding to tuna apomyoglobin measured with fluorescence correlation spectroscopy. Biophys. J. **81:** 3510–3521
84 Henriksson M., Pramanik A., Shafqat J., Zhong Z., Tally M., Ekberg K. et al. (2001) Specific binding of proinsulin C-peptide to intact and to detergent-solubilized human skin fibroblasts. Biochem. Biophys. Res. Commun. **280:** 423–427
85 Zhong Z.-H., Pramanik A., Ekberg K., Jansson O. T., Jörnvall H., Wahren J. et al. (2001) Insulin binding monitored by fluorescence correlation spectroscopy. Diabetologia **44:** 1184–1188
86 Korn K., Gardellin P., Liao B., Amacker M., Bergström Å., Björkman H. et al. (2003) Gene expression analysis using single molecule detection. Nucleic Acids Res. **31:** e89
87 Kunath K., Merdan T., Hegener O., Häberlein H. and Kissel T. (2003) Integrin targeting using RGD-PEI conjugates for in vitro gene transfer. J. Gene Med. **5:** 588–599
88 Clamme J. P., Krishnamoorthy G. and Mély Y. (2003) Intracellular dynamics of the gene delivery vehicle polyethylenimine during transfection: investigation by two-photon fluorescence correlation spectroscopy. Biochim. Biophys. Acta **1617:** 52–61
89 Wennmalm S., Edman L. and Rigler R. (1997) Conformational fluctuations in single DNA molecules. Proc. Natl. Acad. Sci. USA **94:** 10641–10646
90 Edman L., Földes-Papp Z., Wennmalm S. and Rigler R. (1999) The fluctuating enzyme: a single molecule approach. Chem. Phys. **247:** 11–22
91 Edman L. and Rigler R. (2000) Memory landscapes of single-enzyme molecules. Proc. Natl. Acad. Sci. USA **97:** 8266–8271

92 Yang H., Luo G., Karnchanaphanurach P., Louie T.-M., Rech I., Cova S. et al. (2003) Protein conformational dynamics probed by single-molecule electron transfer. Science **302:** 262–266
93 Haupts U., Maiti S., Schwille P. and Webb W. W. (1998) Dynamics of fluorescence fluctuations in green fluorescent protein observed by fluorescence correlation spectroscopy. Proc. Natl. Acad. Sci. USA **95:** 13573–13578
94 Vlad M. O., Moran F., Schneider F. W. and Ross J. (2002) Memory effect and oscillations in single-molecule kinetics. Proc. Natl. Acad. Sci. USA **99:** 12548–12555
95 Copley D. S. (2003) Enzymes with extra talents: moonlighting functions and catalytic promiscuity. Curr. Opin. Chem. Biol. **7:** 265–272
96 James L. C. and Tawfik D. S. (2003) Conformational diversity and protein evolution – a 60-year-old hypothesis revisited. Trends Biochem. Sci. **28:** 361–368
97 Frauenfelder H., Sligar S. G. and Wolynes P. G. (1991) The energy landscapes and motions of proteins. Science **254:** 1598–1603
98 Frauenfelder H., McMahon B. H., Austin R. H., Chu K. and Groves J. T. (2001) The role of structure, energy landscape, dynamics and allostery in the enzymatic function of myoglobin. Proc. Natl. Acad. Sci. USA **98:** 2370–2374
99 James L. C., Roversi P. and Tawfik D. S. (2003) Antibody multispecifity mediated by conformational diversity. Science **299:** 1362–1367
100 Bryngelson J., Onuchic J., Socci N. and Wolynes P. (1995) Funnels, pathways and the energy landscape of protein folding: a synthesis. Proteins Struct. Funct. Genet. **21:** 167–195
101 Licht S. S., Sonnleitner A., Weiss S. and Schultz P. G. (2003) A rugged energy landscape mechanism for trapping of transmembrane receptors during endocytosis. Biochemistry **42:** 2916–2925
102 Yakovleva T., Pramanik A., Kawasaki T., Tan-No K., Gileva I., Lindegren H. et al. (2001) p53 latency: C-terminal domain prevents binding of p53 core to target but not to nonspecific DNA sequences. J. Biol. Chem. **276:** 15650–15658
103 Yakovleva T., Pramanik A., Terenius L., Ekström T. and Bakalkin G. (2002) p53 latency – out of the blind alley. Trends Biochem. Sci. **27:** 612–618
104 Vukojević V., Yakovleva T. and Bakalkin G. (2005) Modes of p53 interactions with DNA in the chromatin context. In: The p53 pathway, Hupp T. and Ayed A. (ed.), Landes Bioscience, Georgetown, in press
105 Johnson R. A., Ince T. A. and Scotto K. W. (2001) Transcriptional repression by p53 through direct binding to a novel DNA element. J. Biol. Chem. **276:** 27716–27720
106 D'Souza S., Xin H., Walter S. and Choubey D. (2001) The gene encoding p202, an interferon-inducible negative regulator of the p53 tumor suppressor, is a target of p53-mediated transcriptional repression. J. Biol. Chem. **276:** 298–305
107 Hoffman W. H., Biade S., Zilfou J. T., Chen J. and Murphy M. (2002) Transcriptional repression of the anti-apoptotic *survivin* gene by wild type p53. J. Biol. Chem. **277:** 3247–3257
108 Murphy M., Ahn J., Walker K. K., Hoffman W. H., Evans R. M., Levine A. J. et al. (1999) Transcriptional repression by wild-type p53 utilizes histone deacetylases, mediated by interaction with mSin3a. Genes Dev. **13:** 2490–2501
109 Zilfou J. T., Hoffman W. H., Sank M., George D. L. and Murphy M. (2001) The corepressor mSin3a interacts with the proline-rich domain of p53 and protects p53 from proteasome-mediated degradation. Mol. Cell. Biol. **21:** 3974–3985
110 Wang T., Kobayashi T., Takimoto R., Denes A. E., Snyder E. L., el-Deiry W. S. et al. (2001) hADA3 is required for p53 activity. EMBO J. **20:** 6404–6413
111 Ard P. G., Chatterjee C., Kunjibettu S., Adside L. R., Gralinski L. E. and McMahon S. B. (2002) Transcriptional regulation of the *mdm2* oncogene by p53 requires TRRAP acetyltransferase complexes. Mol. Cell. Biol. **22:** 5650–5661
112 Langley E., Pearson M., Faretta M., Bauer U.-M., Frye R. A., Minucci S. et al. (2002) Human SIR2 deacetylates p53 and antagonizes PML/p53-induced cellular senescence. EMBO J. **21:** 2383–2396
113 Ruan Q., Chen Y., Gratton E., Glaser M. and Mantulin W. W. (2002) Cellular characterization of adenylat kinase and its isoform: two-photon excitation fluorescence imaging and fluorescence correlation spectroscopy. Biophys. J. **83:** 3177–3187
114 Saito K., Ito E., Takakuwa Y., Tamura M. and Kinjo M. (2003) In situ observation of mobility and anchoring of PKCβI in plasma membrane. FEBS Lett. **541:** 126–131
115 Korlach J., Schwille P., Webb W. W. and Feigenson G. W. (1999) Characterization of lipid bilayer phases by confocal microscopy and fluorescence correlation spectroscopy. Proc. Natl. Acad. Sci. USA **96:** 8461–8466
116 Schwille P. Korlach J. and Webb W. W. (1999) Fluorescence correlation spectroscopy with single-molecule sensitivity on cell and model membranes. Cytometry **36:** 176–182
117 Kues T., Peters R. and Kubitscheck U. (2001) Visualisation and tracking of single protein molecules in the cell nucleus. Biophys. J. **80:** 2954–2967
118 Pramanik A. (2004) Molecular interaction of peptides with phospholipid membranes by fluorescence correlation spectroscopy. In: Recent Research Developments in Chemistry and Physics of Lipids, pp. 53–70, Pandalai S. G. (ed.), Transworld Research Network, Trivandrum
119 Sorcher S. M., Bartholomew J. C. and Klein M. P. (1980) The use of fluorescence correlation spectroscopy to probe chromatin in the cell nucleus. Biochim. Biophys. Acta **610:** 28–46
120 Politz J. C., Browne E. S., Wolf D. E. and Pederson T. (1998) Intranuclear diffusion and hybridisation state of oligonucleotides measured by fluorescence correlation spectroscopy in living cells. Proc. Natl. Acad. Sci. USA **95:** 6043–6048
121 Wachsmuth M., Waldeck W. and Langovski J. (2000) Anomalous diffusion of fluorescent probes inside living cell nuclei investigated by spatially-resolved fluorescence correlation spectroscopy. J. Mol. Biol. **298:** 677–689
122 Wachsmuth M., Weidemen T., Müller G., Hoffman-Rohrer U. W., Knoch,T. A., Waldeck W. et al. (2003) Analyzing intracellular binding and diffusion with continuous fluorescence photobleaching. Biophys. J. **84:** 3353–3363
123 Elowitz M. B., Surette M. G., Wolf P.-E., Sock J. B. and Leibler S. (1999) Protein mobility in the cytoplasm of *Escherichia coli*. J. Bacteriol. **181:** 197–203
124 Ellis R. J. (2001). Macromolecular crowding: obvious but underappreciated. Trends Biochem. Sci. **26:** 597–604
125 Francke C., Postma P. W., Westerhoff H. V., Blom J. G. and Peletier M. A. (2003) Why the Phosphotransferase system of *Escherichia coli* escapes diffusion limitation. Biophys. J. **85:** 612–622
126 Goldbeter A. (2002) Computational approaches to cellular rhythms. Nature **420:** 238–245
127 Gonze D., Halloy J. and Goldbeter A. (2002) Robustness of circadian rhythms with respect to molecular noise. Proc. Natl. Acad. Sci. USA **99:** 673–678
128 Qi S. Y., Groves J. T. and Chakraborty A. K. (2001) Synaptic pattern formation during cellular recognition. Proc. Natl. Acad. Sci. USA **98:** 6548–6553
129 Schnell S., Maini P. K., McInerney D., Gavaghan D. J. and Houston P. (2002) Models for pattern formation in somitogenesis: a marriage of cellular and molecular biology. C. R. Biologies **325:** 179–189
130 Endy D. and Brent R. (2001) Modelling cellular behaviour. Nature **409:** 391–395
131 Phair R. D. and Misteli T. (2001) Kinetic modelling approaches in in vivo imaging. Nat. Rev. Mol. Cell Biol. **2:** 898–907
132 Hlavacek W. S., Redondo A., Wofsy C. and Goldstein B. (2002) Kinetic proofreading in receptor-mediated transduc-

tion of cellular signals: receptor aggregation, partially activated receptors, and cytosolic messengers. Bull. Math. Biol. **64:** 887–911
133 Köhler R., Schwille P., Webb W. W. and Hanson M. R. (2000) Active protein transport through plastide tubules: velocity quantified by fluorescence correlation spectroscopy. J. Cell. Sci. **113:** 3921–3930
134 Lippitz M., Erker W., Decker H., van Holde K. E. and Basché T. (2002) Two-photon excitation microscopy of tryptophan-containing proteins. Proc. Natl. Acad. Sci. USA **99:** 2772–2777
135 Weijer C. J. (2003) Visualizing signals moving in cells. Science **300:** 96–100
136 Widengren J. and Rigler R. (1998) Fluorescence correlation spectroscopy as a tool to investigate chemical reactions in solutions and on cell surfaces, Cell. Mol. Biol. **44:** 857–879
137 Pramanik A., Juréus A., Langel Ü., Bartfai T. and Rigler R. (1999) Galanin receptor binding in the membranes of cultured cells measured by fluorescence correlation spectroscopy, Biomed. Chromatogr. **13:** 119–121
138 Rigler R., Pramanik A., Jonasson P., Kratz G., Jansson O., Nygren P.-Å. et al. (1999) Specific binding of proinsulin C-peptide to human cell membranes, Proc. Natl. Acad. Sci. USA **96:** 13318–13323
139 Boonen G., Pramanik A., Rigler R. and Häberlein H. (2000) Evidence for specific interactions between a kavain derivative and human cortical neurons measured by fluorescence correlation spectroscopy. Planta Med. **66:** 7–10
140 Pramanik A., Thyberg P. and Rigler R. (2000) Molecular interactions of peptides with phospholipid vesicle membranes as studied by fluorescence correlation spectroscopy, Chem. Phys. Lipids **104:** 35–47
141 Pramanik A., Juréus A., Langel Ü., Bartfai T. and Rigler R. (2001) Fluorescence correlation spectroscopy detects galanin receptor diversity on insulinoma cells. Biochemistry **40:** 10839–10845
142 Pramanik A. and Rigler R. (2001) Ligand-receptor interactions in the membrane of cultured cells monitored by fluorescence correlation spectroscopy. Biol. Chem. **382:** 371–378
143 Pramanik A. and Rigler R. (2001) FCS-assay of ligand-receptor interactions in living cells. In: Fluorescence Correlation Spectroscopy (FCS). Theory and Applications, pp. 101–129, Rigler R. and Elson E. L. (eds), Springer, Berlin
144 Pramanik A., Ekberg K., Zhong Z., Shafqat J., Henriksson M., Jansson O. et al. (2001) C-peptide binding to human cell membranes: Importance of Glu27, Biochem. Biophys. Res. Commun. **284:** 94–98
145 Pramanik A. (2004) Ligand-receptor interaction in live cells by fluorescence correlation spectroscopy. Current Pharm. Biotech. **5:** 205–212
146 Meissner O. and Häberlein H. (2003) Lateral mobility and specific binding to $GABA_A$ receptors on hippocampal neurons monitored by fluorescence correlation spectroscopy. Biochemistry **42:** 1667–1672
147 Patel R. C., Kumar U., Lamb D. C., Eid J. S., Rocheville M., Grant M et al. (2002) Ligand binding to somatostatin receptors induces receptor-specific oligomer formation in live cells. Proc. Natl. Acad. Sci. USA **99:** 3294–3299
148 Kahya N., Scherfeld D., Bacia K., Poolman B. and Schwille P. (2003) Probing lipid mobility of raft-exhibiting model membranes by fluorescence correlation spectroscopy. J. Biol. Chem. **278:** 28109–28115
149 Reznikov K., Kolesnikova L., Pramanik A., Tan-No K., Gileva I., Yakovleva T. et al. (2000) Clustering of apoptotic cells via bystander killing by peroxides. FASEB J. **14:** 1754–1764
150 Narayanan P. K., Goodwin E. H. and Lehnert B. E. (1997) Alpha particles initiate biological production of superoxide anions and hydrogen peroxide in human cells. Cancer Res. **57:** 3963–3971
151 Mothersill C. and Seymour C. B. (1998) Cell-cell contact during gamma irradiation is not required to induce a bystander effect in normal human keratinocytes: evidence for release during irradiation of a signal controlling survival into the medium. Radiation Res. **149:** 256–262
152 Prise K. M., Belyakov O. V., Folkard M. and Michael B. D. (1998) Studies of bystander effects in human fibroblasts using a charged particle microbeam. Int. J. Rad. Biol. **74:** 793–798
153 Nathan C. F. (1987) Neutrophil activation on biological surfaces. Massive secretion of hydrogen peroxide in response to products of macrophages and lymphocytes. J. Clin. Invest. **80:** 1550–1560
154 Van Dissel J. T., Stikkelbroeck J. J., Michael B. C., Leijh C. and Furth R. (1987) Salmonella-typhimurium-specific difference in rate of intracellular killing by resident peritoneal macrophages from salmonella-resistant CBA and salmonella-susceptible C57BL/10 mice. J. Immunol. **138:** 4428–4434
155 Maxeiner H., Husemann J., Thomas C. A., Loike J. D., El Khoury J. and Silverstein S. C. (1998) Complementary roles for scavanger receptors A and CD36 of human monocyte-derived macrophages in adhesion to surfaces coated with oxidized low-density lipoproteins and in secretion of H_2O_2. J. Exp. Med. **188:** 2257–2265
156 Tjernberg L. O., Pramanik A., Bjorling S., Thyberg P., Thyberg J., Nordstedt et al. (1999) Amyloid beta-peptide polymerization studied using fluorescence correlation spectroscopy. Chem. Biol. **6:** 53–62
157 Lagerkvist A. C., Földes-Papp Z., Persson M. A. A. and Rigler R. (2001) Fluorescence correlation spectroscopy as a method for assessment of interactions between phage displaying antibodies and soluble antigen. Protein Sci. **10:** 1522–1528
158 Földes-Papp Z., Demel U., Domej W. and Tilz G. P. (2002) A new dimension for the development of fluorescence-based assays in solution: from physical principles of FCS detection to biological applications. Exp. Biol. Med. **227:** 291–300
159 Földes-Papp Z., Demel U. and Tilz G. P. (2002) Detection of single molecules: solution-phase single-molecule fluorescence correlation spectroscopy as an ultrasensitive, rapid and reliable system for immunological investigation. J. Immunol. Methods **260:** 117–124
160 Kettling U., Koltermann A., Schwille P. and Eigen M. (1998) Real-time enzyme kinetics monitored by dual-color fluorescence cross-correlation spectroscopy. Proc. Natl. Acad. Sci. USA **95:** 1416–1420
161 Koltermann A., Kettling U., Bieschke J., Winkler T. and Eigen M. (1998) Rapid assay processing by integration of dual-color fluorescence cross-correlation spectroscopy: high throughput screening for enzyme activity. Proc. Natl. Acad. Sci. USA **95:** 1421–1426
162 Amedek A., Haustein E., Scherfeld D. and Schwille P. (2002) Scanning dual-color cross-correlation analysis for dynamic co-localization studies of immobile molecules. Single Mol. **3:** 201–210
163 Bacia K., Majoul I. V. and Schwille P. (2002) Probing the endocytic pathway in live cells using dual-color fluorescence cross-correlation analysis. Biophys. J. **83:** 1184–1193
164 Heinze K. G., Rarbach M., Jahnz M. and Schwille P. (2002) Two-photon fluorescence coincidence analysis: rapid measurements of enzyme kinetics. Biophys. J. **83:** 1671–1681
165 Hom E. F. Y. and Verkman A. S. (2002) Analysis of coupled bimolecular reaction kinetics and diffusion by two-color fluorescence correlation spectroscopy: enhanced resolution of kinetics by resonance energy transfer. Biophys. J. **83:** 533–546
166 Chen Y., Müller J. D., Ruan Q. Q. and Gratton E. (2002) Molecular brightness characterization of EGFP in vivo by fluorescence fluctuation spectroscopy. Biophys. J. **82:** 133–144
167 Palo K., Brand L., Eggeling C., Jäger S., Kask P. and Gall K. (2002) Fluorescence intensity and lifetime distribution analy-

sis: toward higher accuracy in fluorescence fluctuation spectroscopy. Biophys. J. **83:** 605–618
168 Starr T. and Thompson N. L. (2001) Total internal reflection with fluorescence correlation spectroscopy: combined surface reaction and solution diffusion. Biophys. J. **80:** 1575–1584
169 Dombeck D. D., Kasischke K. A., Vishwasrao H. D., Ingelsson M., Hyman B. T. and Webb W. W. (2003) Uniform polarity microtubule assemblies imaged in native brain tissue by second harmonic generation microscopy. Proc. Natl. Acad. Sci. USA **100:** 7081–7086
170 Czerney P., Lehmann F., Wenzel M., Buschmann V., Dietrich A. and Mohr G. J. (2001) Tailor-made dyes for fluorescence correlation spectroscopy (FCS). Biol. Chem. **382:** 495–498
171 Dittrich P., Malvezzi-Campeggi F., Jahnz M. and Schwille P. (2001) Accessing molecular dynamics in cells by fluorescence correlation spectroscopy. Biol. Chem. **382:** 491–494
172 Widengren J., Terry T. and Rigler R. (1999) Protonation kinetics of GFP and FITC investigated by FCS-aspects of the use of fluorescent indicators for measuring pH. Chem. Phys. **249:** 259–271
173 Widengren J., Mets Ü. and Rigler R. (1999) Photodynamic properties of green fluorescent proteins investigated by fluorescence correlation spectroscopy. Chem. Phys. **250:** 171–186
174 Schwille P., Kummer S., Heikal A. A., Moerner W. E. and Web W. W. (2000) Fluorescence correlation spectroscopy reveals fast optical excitation-driven intramolecular dynamics of yellow fluorescent protein. Proc. Natl. Acad. Sci. USA **97:** 151–156
175 Zhang J., Campbell R. E., Ting A. Y. and Tsien R. Y. (2002) Creating new fluorescent probes for cell biology. Nat. Rev. Mol. Cell Bio. **3:** 906–918
176 Delon A., Usson Y., Derouard J., Biben T. and Souchier S. (2004) Photobleaching, mobility and compartmentalization: inferences in fluorescence correlation spectroscopy. J. Fluoresc. **14:** 255–267
177 Brock R., Hink M. A. and Jovin T. M. (1998) Fluorescence correlation microscopy of cells in the presence of autofluorescence. Biophys. J. **75:** 2547–2557
178 Gennerich A. and Schild D. (2000) Fluorescence correlation spectroscopy in small cytosolic compartments depends critically on the diffusion model used. Biophys. J. **79:** 3294–3306
179 Brown F. L. H. (2003) Regulation of protein mobility via thermal membrane undulations. Biophys. J. **84:** 842–853
180 Fradin C., Abu-Arish A., Granek R. and Elbaum M. (2003) Fluorescence correlation spectroscopy close to a fluctuating membrane. Biophys. J. **84:** 2005–2020

Appendix

Intensity detection function

For the confocal setup and the laser beam profile that are common in today's equipment, the detection volume within the confocal volume element from which fluorescence is being detected can be approximated by an ellipsoid (fig. 1) [21, 22]. The intensity detection function from this ellipsoid volume element can be expressed in the following form:

$$I(x,y,z) = I\sigma\phi_f \kappa \exp\left(\frac{-2(x^2+y^2)}{w_{xy}^2} - \frac{2z^2}{w_z^2}\right) \quad (6)$$

In equation (6), I is maximal intensity of the laser light beam, σ is the optical absorption cross section, ϕ_f is the fluorescence quantum yield of the applied dye, κ is the maximum value of the light collection efficiency, x and y are coordinates perpendicular to the optical axis, z is a coordinate along the optical axis (along which the laser beam propagates), w_{xy} and w_z are radial and axial parameters, respectively, related to spatial properties of the detection volume.

Autocorrelation functions

Prior to taking FCS measurements, it is very important to take notice of processes (free and anomalous diffusion, active transport, intracellular compartmentalization, chemical reactions, photophysical processes etc.) that may lead to fluctuations in the fluorescence signal, because all processes leading to statistical fluctuations in the fluorescence signal will induce a characteristic decay time in the autocorrelation curve. Only then can one select a proper theoretical correlation function to model the experimental data and be assured that they are accurately interpreted. In table A, we give examples of autocorrelation functions for several different model systems that are relevant in biochemical investigations.

Special requirements related to FCS application in biological systems

When FCS measurements are to be performed in biological systems, it is very important to be aware of distinctive properties of these systems that may lead, when not properly accounted for, to erroneous interpretation of FCS data. Therefore, we would like to draw attention to the most common obstacles that may cause a faulty interpretation of FCS measurements in biological systems. As many potential sources of errors are already recognized and well characterized, we shall just point them out here, and we direct the readers to references describing in detail how to avoid and resolve such problems.

1) In many applications of FCS the exobiotic under investigation is not intrinsically fluorescent, and hence has to be labelled with a fluorophore. Addition of a fluorophore may change the biological and/or physicochemical properties of the substance in such a way that it no longer shows characteristics of the parental compound [170, 171]. Therefore, fluorescent probes have to be selected carefully to induce minimal perturbation in the system under investigation [34, 172–175]. In addition, when FCS is applied under single-photon excitation, the fluorescent reporter may become prone to irreversible photobleaching because it cannot withstand the high-intensity irradiation in the laser focus. This may strongly alter the shape of the autocorrelation curve and hence lead to erroneous data interpretation (e.g. [7, 163]). Typically, this problem is resolved by optimizing experimental conditions to avoid strong photobleaching, i.e. by selecting more stable fluorophores and working with lower-intensity laser power. However, attempts have been made recently to take advantage of this phenomenon and extract information about spatial compartmentalization [176].

2) Interpretation of the FCS measurements is susceptible to errors arising from background scattering and fluorescence, photon shot noise and excitation power instabilities. Their effect has to be carefully considered and accounted for to meet the specific requirements for FCS applications in biological systems [29, 45, 116, 177].

3) It is very important to realize that the experimentally determined correlation function, which in practice has to be calculated from a finite data set, can only be regarded as a statistical estimation of the theoretical correlation function. To avoid significant systematic deviation of the experimentally determined correlation function from the theoretical ensemble average, it is very important to perform measurements for a sufficiently long time and to average them over an adequate number of repeats. Or, if it is not possible to perform long time measurements, as is often the case with living cells, one has to know how to estimate the bias and how to correct the experimental autocorrelation function [54].

4) When FCS measurements are to be carried out to characterize cellular processes, application of standard FCS autocorrelation functions, in forms given in table A, may sometime lead to erroneous results. There may be several reasons for such deviations.

Table A. Examples of autocorrelation functions for different model systems relevant in biochemical investigations.

AF1 Two-dimensional diffusion of a single fluorescent species

$$G(\tau)=1+\frac{1}{N}\cdot\frac{1}{\left(1+\frac{\tau}{\tau_D}\right)}$$

AF2 Free diffusion of a single species and triplet formation

$$G(\tau)=1+\frac{1}{N}\cdot\frac{1}{\left(1+\frac{\tau}{\tau_D}\right)\sqrt{1+\frac{w_{xy}^2}{w_z^2}\frac{\tau}{\tau_D}}}\cdot\left[1+\frac{T}{1-T}\exp-\left(\frac{\tau}{\tau_T}\right)\right]$$

T, average equilibrium fraction of molecules in triplet state
τ_T, triplet correlation time, related to rate constants for intersystem crossing and the triplet decay

AF3 Free diffusion of unbound ligand and the ligand-receptor complex

$$G(\tau)=1+\frac{1}{N}\cdot\left(\frac{1-y}{\left(1+\frac{\tau}{\tau_{D1}}\right)\sqrt{1+\frac{w_{xy}^2}{w_z^2}\frac{\tau}{\tau_{D1}}}}+\frac{y}{\left(1+\frac{\tau}{\tau_{D2}}\right)\sqrt{1+\frac{w_{xy}^2}{w_z^2}\frac{\tau}{\tau_{D2}}}}\right)$$

y, fraction of ligand bound to the receptor
τ_{D_1}, diffusion time of the unbound ligand
τ_{D_2}, diffusion time of the bound ligand

AF4 Free diffusion of unbound ligand and diffusion of a ligand bound to a surface

$$G(\tau)=1+\frac{1}{N}\cdot\left(\frac{1-y}{\left(1+\frac{\tau}{\tau_{D1}}\right)\sqrt{1+\frac{w_{xy}^2}{w_z^2}\frac{\tau}{\tau_{D1}}}}+\frac{y}{\left(1+\frac{\tau}{\tau_{D2}}\right)}\right)$$

y, fraction of bound ligand
τ_{D_1}, diffusion time of the unbound ligand
τ_{D_2}, diffusion time of the bound ligand

AF5 Concentration fluctuations around a chemical equilibrium coupled with diffusion

$$G(\tau)=1+\frac{1}{N(1-F)}\cdot\frac{1}{\left(1+\frac{\tau}{\tau_D}\right)\sqrt{1+\frac{w_{xy}^2}{w_z^2}\frac{\tau}{\tau_D}}}\cdot\left[1-F+F\exp\left(\frac{-\tau}{\tau_C}\right)\right]$$

The chemical reaction analyzed is AB $\Leftrightarrow$ A* + B; A* is the only fluorescent species
F, average fraction of molecules in the non-fluorescent state AB
τ_C, chemical relaxation time from which rate constants are derived

AF6 Restricted (anomalous) diffusion due to interactions with fixed or mobile structures

$$G(\tau)=1+\frac{1}{N}\cdot\frac{1}{\left(1+\left(\frac{\tau}{\tau_D}\right)^{\alpha}\right)\sqrt{1+\frac{w_{xy}^2}{w_z^2}\left(\frac{\tau}{\tau_D}\right)^{\alpha}}}$$

α, restriction coefficient; for free (Brownian) diffusion $\alpha = 1$, and for restricted diffusion $\alpha < 1$

Table A (continued)

AF7 Active transport

$$G(\tau) = 1 + \frac{1}{N} \cdot \exp\left(-\left(\tau \cdot \frac{v}{w_{xy}} \right)^2 \right)$$

v, velocity of active radial transport

AF8 Mixed mode diffusion – active transport coupled with diffusion

$$G(\tau) = 1 + \frac{1}{N} \cdot \frac{1}{\left(1+\frac{\tau}{\tau_D}\right)\sqrt{1+\frac{w_{xy}^2}{w_z^2}\frac{\tau}{\tau_D}}} \cdot \exp\left(-\left(\tau \cdot \frac{v}{w_{xy}} \right)^2 \cdot \frac{1}{\left(1+\frac{\tau}{\tau_D}\right)} \right)$$

- **Detection volume may be confined by intracellular compartmentalization rather than by the geometry of the optical setup.** In the derivation of standard autocorrelation functions (table A) it is assumed that the volume within which diffusion occurs is much larger than the confocal volume element in which fluorescence is being recorded. This may not be true for living cells where, due to different morphological properties of the cell, the detection volume may be of the same size or smaller than the confocal volume element. In addition, inside a living cell the volume in which fluorescence is being detected need not have the ellipsoid-like shape given by equation (6), but may be altered by presence of membranes or cell particles [178].

- **Diffusion pattern through a volume element may be distorted by a nearby obstacle.** If a particle bounces back from a nearby obstacle, a membrane or large cell particle, for example, it may immediately re-enter the detection volume. This will be reflected in FCS measurements as an increased residence time, i.e. as an increased characteristic decay time τ_D, and may be wrongly interpreted and associated with a smaller diffusion coefficient and, hence, with a larger particle size.

- **Diffusion properties depend on physicochemical characteristics of nearby membranes.** Intracellular structures are usually bound by soft lipidic membranes undergoing thermally driven mechanical fluctuations [179]. Innate fluctuations of a nearby membrane may modify the geometry of the detection volume and/or the number of particles in the detection volume, and hence will reverberate in FCS measurements [52, 180]. Thus, autocorrelation functions AF4, AF6 and AF8, in the form given in table A, can be applied to describe diffusion in standard, unconfined, detection volumes and binding to a single rigid membrane, whereas these approximations are no longer valid in the case of confined detection volumes, restricted diffusion in one dimension (diffusion between two rigid membranes) and diffusion close to membranes undergoing mechanical fluctuations. In such cases, the autocorrelation functions ought to be augmented to account for the particulars [180]. In addition to membrane composition [148], its local morphology, i.e. its shape, and orientation with respect to the observation volume may be reflected in FCS measurements, and have to be accounted for in a correct interpretation of FCS data [52, 53].